DOI 10.1007/s11141-023-10280-w
Radiophysics and Quantum Electronics, Vol. 66, Nos. 2–3, July–August, 2023
(Russian Original Vol. 66, Nos. 2–3, February–March, 2023)

TWO WAYS TO GENERALIZE GERSTNER WAVES IN THE THEORY OF WAVES IN DEEP WATER

A. A. Abrashkin [1,2] * **and E. N. Pelinovsky** [1,2]

UDC 532.59-3

By convention, water waves are studied under the assumption of their potentiality. This approximation is not always valid in natural conditions. The vorticity is introduced by shear currents, which are ubiquitous in the ocean. It is also generated in the near-surface layer as a result of wind action. When these factors are taken into account, the models developed for potential waves require refinement and generalization. This paper is devoted to a review of advances in the field of analytical description of surface vortical waves in deep water. The presentation is based on the Lagrangian approach. The focus is on the Gerstner wave, a particular exact solution of the Euler equation. Two ways of its generalization are discussed. The first suggests consideration of weakly nonlinear steady waves with a more general vorticity distribution (Gouyon waves). The second way is to construct exact solutions for waves with inhomogeneous and non-stationary pressure distribution on a free surface (generalized Gerstner waves).

1. INTRODUCTION

The advent of science about nonlinear waves is conventionally related to the first experiments of S. Russell, who observed for the first time solitons moving along a shallow channel surface [1] in the 1830s–1840s. In 1895, Korteweg and de Vries gave a mathematical description of this phenomenon based on an equation that was later named after them [2]. However, the historically first analytical representation for a nonlinear wave, which was published by F. J. Gerstner at the beginning of the XIX century and described a stationary wave in deep water with a trochoid-shaped profile, remained (and still remains) out of sight for many researchers [3, 4]. Due to a number of circumstances, which are discussed in what follows, the Gerstner wave did not receive even one-thousandth of attention that was paid to the Korteweg—de Vries solitons. But the fact that the Gerstner wave was the first remains.

The weakly nonlinear Stokes wave [5] also became more popular and attracted much greater attention in comparison with the Gerstner wave. This circumstance, at first glance, looks even more surprising, since the Stokes solution is written as a series in terms of the small wave steepness parameter. Such a representation for a periodic surface wave turned out to be more important for practical purposes than the exact solution. The reason is the problem of implementing the Gerstner wave. In contrast to the Stokes wave, it is a vortex wave and cannot occur in nature under the action of potential forces (Lagrange theorem). In order to implement the Gerstner wave, either the action of external non-potential forces or special initial conditions are necessary. Thus, H. Lamb suggested that the Gerstner wave can occur from a shear current having the same vorticity as the wave [4]. In this case, the translational motion of fluid particles in the flow should be transformed into circular rotation (there is no drift current in the Gerstner wave). The specificity of such

* aabrashkin@hse.ru

[1] Higher School of Economics; [2] Institute of Applied Physics of the Russian Academy of Sciences, Nizhny Novgorod, Russia. Translated from Izvestiya Vysshikh Uchebnykh Zavedenii, Radiofizika, Vol. 66, Nos. 2–3, pp. 130–144, February–March 2023. Russian DOI: 10.52452/00213462_2023_66_02_130 Original article submitted December 22, 2022; accepted May 28, 2023.

a scenario clearly did not contribute to the popularization of the Gerstner solution and its wide application for practical calculations. Nevertheless, A. N. Krylov developed a theory of ship rolling in a rough sea based on Gerstner's formulas [6], which found great application in shipbuilding [7]. Dubreil-Jacotin showed that Gerstner waves can exist in a fluid with arbitrary stratification [8].

The discovery of the mechanism of modulation instability for potential waves on water [9], one would think, finally turned Gerstner's theory into a hydrodynamic artifact, i. e., a beautiful exact solution, impossible to obtain in nature, but all of a sudden, from about the same time, examples of its new applications began to appear. Pollard modified the Gerstner solution for waves in a rotating fluid in the f-plane approximation [10]. Yih [11], Mollo-Christensen [12, 13], and, in a more complete form, Constantin [14] applied Gerstner's solution to describe edge waves propagating along a sloping beach (these works have shown that the results for a homogeneous fluid can be generalized to the case of fluid stratification and rotation). In addition to this, Mollo-Christensen gave a description of Gerstner wave bores (trochoidal clouds) in a stratified atmosphere [15], and the authors of [16] and [17] found a cylindrical analogue of Gerstner waves, namely, epicycloidal waves moving along the free surface of a cavity in a uniformly rotating fluid.

These achievements significantly increased the status of Gerstner's solution, but the question about its physical implementation was still open. This long-standing problem, however, was solved by Monismith and co-authors [18], who managed to create a Gerstner wave in laboratory conditions. The principle of the experiment was as follows. In the Gerstner wave, fluid particles move in a circle, and, therefore, no drift current takes place in it. This distinguishes it from the Stokes wave, the propagation of which is accompanied by particle transport (Stokes drift). This drift is directed along the wave motion; thus, when a Gerstner wave was generated, a current moving in the opposite direction was created. The absence of drift of fluid particles during the observation of a separate implementation witnessed the recording of a Gerstner wave in the experiment. It is necessary to emphasize the particular thoroughness with which the authors of [18] formulated their conclusions. For their additional verification, they addressed similar experiments conducted in other laboratories and showed that Gerstner waves were observed earlier in three of them [19–21].

All of these results were obtained in bounded channels with artificially (mechanically) generated waves. But, as the authors of [18] note, a similar observation (i. e., the absence of drift of fluid particles) was also recorded for waves in the open ocean [22]. Thus, the existence of Gerstner waves was also confirmed by *in-situ* observations. With a steepness exceeding $1/3$, Gerstner waves are unstable to three-dimensional perturbations [23], but it has now become possible to talk about them as real physical oscillations. In turn, Weber pointed out that with allowance for the viscosity and surface films, a drift flow occurs in the Gerstner wave [24]. Such wave oscillations, in his opinion, could well (without recognizing this fact and linking to Gerstner waves) have been observed by experimenters in laboratory pools for a long time.

This paper discusses two ways of generalizing Gerstner waves. The first one is related to the description of weakly nonlinear stationary waves with a more general distribution of vorticity, which is given as a series in terms of the small wave steepness parameter. The second way suggests the deriving of a family of exact solutions, for which the pressure on a free surface is no longer constant and is given by a function that is inhomogeneous in horizontal coordinate and harmonically varies in time. Both approaches, as well as Gerstner's solution itself, are based on the use of Lagrange variables, which allows them to be represented in a unified mathematical context.

2. GERSTNER WAVES

Consider gravity surface waves in a homogeneous fluid. Figure 1 shows the problem geometry and indicates possible boundary conditions on a free surface in the Lagrangian formulation.

The equations of two-dimensional hydrodynamics in the Lagrange variables a and b in the gravity field have the following form [4, 25, 26]:

$$\frac{D(X,Y)}{D(a,b)} = D_0(a,b);$$

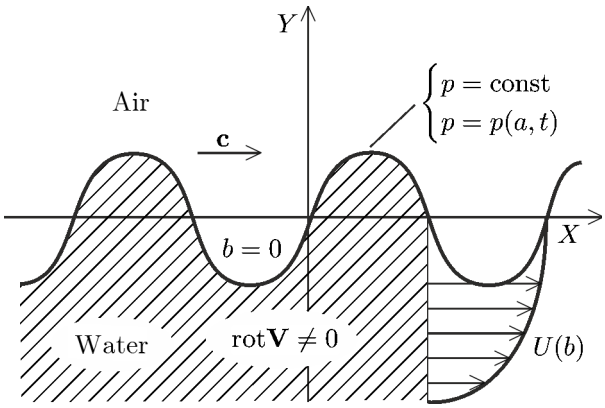

Fig. 1. Geometry of the problem for vortex waves at the water—air boundary. a and b are the Lagrangian variables, $U(b)$ is the vertically inhomogeneous drift of fluid particles, and c is the wave velocity. Pressure on a free surface can be specified both as constant and as inhomogeneous and non-stationary (wind action simulation).

$$X_{tt}X_a + (Y_{tt} + g)Y_a = -\frac{1}{\rho}p_a,$$
$$X_{tt}X_b + (Y_{tt} + g)Y_b = -\frac{1}{\rho}p_b. \qquad (1)$$

Here, $X(a, b, t)$ and $Y(a, b, t)$ are the coordinates of the fluid particle trajectory, t is the time, g is the free-fall acceleration, p is the pressure, ρ is the density, and the subscripts mean differentiation with respect to the corresponding variable. The function D_0 depends on how the particles are labeled. The b axis is directed upwards and $b = 0$ corresponds to a free surface. In the system of equations (1), the first one is the continuity equation for an incompressible fluid and the other two are equations of motion.

Using cross-differentiation, we exclude pressure from the equations of motion [4, 26, 27]:

$$X_{ta}X_b - X_{tb}X_a + Y_{ta}Y_b - Y_{tb}Y_a = D_0\Omega(a, b). \qquad (2)$$

This equation is equivalent to the equations of fluid motion, but includes the vorticity $\Omega = (\partial Y_t/\partial X) - (\partial X_t/\partial Y)$, which is a function of Lagrange variables only for two-dimensional flows. Gerstner pointed out that Eqs. (1) and (2) are satisfied by the following pair of relations [3]:

$$X = a - A\exp(kb)\sin(ka - \omega t); \qquad Y = b + A\exp(kb)\cos(ka - \omega t); \qquad b \le 0. \qquad (3)$$

They describe a gravity wave on the surface of a fluid with amplitude A, wave number k, and frequency ω, traveling at a constant velocity $c = \omega/k$ to the right. No particle oscillations are present at the bottom ($b \to \infty$). Substituting Eq. (3) into the motion equations, we find the pressure distribution in the wave:

$$p = p_0 - pgb - p/2\omega^2A^2[1 - \exp(^2kb)].$$

On a free surface, the pressure is equal to a constant value p_0. It also follows from the condition of pressure independence of time that the condition $\omega^2 = gk$ (the dispersion relation of the wave) must be fulfilled. This condition is exactly the same as for linear potential waves. The trajectory coordinates of an individual particle satisfy the relation $(X - a)^2 + (Y - b)^2 = A^2\exp(2kb)$, from which it follows that in a fixed reference frame each particle moves in a circle with radius $A\exp(kb)$, as well as in linear Stokes waves. The profile of the Gerstner wave is a trochoid. For $A = k^{-1}$ (the limiting value of the amplitude), the wave has a sharp vertex, and its shape is a cycloid. The angle at the vertex of a Gerstner limit wave is zero [4, 7, 25].

In the 1860s, solution (3) was rediscovered by three authors at once, namely, Froude [28], Rankine [29], and Reech [30]. For more than half a century, Gerstner's classical result was unnoticed. And this characterizes Gerstner as an outstanding scientist who was ahead of time.

The Gerstner wave has a non-zero vorticity (see Eq. (2)):

$$\Omega_{\rm G} = \frac{2k^3A^2c\exp(2kb)}{1 - k^2A^2\exp(2kb)}.$$

Expand this expression into a series over the small wave steepness parameter $\varepsilon = kA$:

$$\Omega_{\rm G} = 2k^3A^2c\exp(2kb)[1 + k^2A^2\exp(2kb)] = \Omega_{\rm G2} + {\rm O}[(kA)^4]. \qquad (4)$$

Here, $\Omega_{G2} = 2k^3A^2c\exp(2kb)$ is the vorticity of the Gerstner wave in the quadratic approximation. In the linear approximation, the Gerstner wave is vortex-free and equivalent to a linear Stokes wave.

Let us continue comparing the two types of waves. The Stokes solution in the second order of perturbation theory can be written as follows [31]:

$$X = a - \varepsilon k^{-1}\exp(kb)\sin k(a-ct) + \varepsilon^2 ct\exp(2kb);$$
$$Y = b + \varepsilon k^{-1}\exp(kb)\cos k(a-ct). \tag{5}$$

The motion of fluid particles is the sum of the oscillatory and drift components. If one assumes the amplitude of the Gerstner wave to be small, the oscillatory motions of fluid particles in Eqs. (3) and (5) will coincide. The difference between the Stokes wave and the Gerstner wave in the quadratic approximation is related to the presence of a drift term in the potential wave (Stokes drift). The Gerstner wave vorticity in this approximation is equal to Ω_{G2} (see Eq. (4)), and the Stokes drift vorticity is determined by the formula

$$\Omega_{Sd} = -2kc\varepsilon^2\exp(2kb) = -\Omega_{G2}.$$

The motion of fluid particles in a Stokes wave consists of the superposition of two currents, namely, rotational in a circle (Gerstner) and shear (Stokes drift). Each current has vorticity, but their total vorticity is zero.

Solution (5) was obtained by Stokes [5]; however, neither Stokes himself nor other researchers reproducing his result correlated the oscillatory part of the solution with the Gerstner wave. In symbolic form, the Stokes result can be written in the form [32]

$$\text{Stokes wave} = \text{Gerstner wave} + \text{Stokes drift}.$$

Despite all the evidence, this result has not been explicitly formulated in the literature. Apparently, this is due to the fact that the solution for the Stokes wave potential is usually written in Euler variables. The Stokes solutions in Lagrange variables, on the contrary, highlights our symbolic formula. First, we emphasize its non-obviousness, and, second, its non-triviality, since the principle of current superposition takes place in the nonlinear approximation. It is interesting to add that the profiles of the Stokes and Gerstner waves coincide up to the cubic approximation with respect to a small steepness parameter [7]. The profiles differ only in the fourth order of perturbation theory.

Let us discuss one more difference between these waves. The dispersion relation for the Gerstner wave does not contain an amplitude, and, therefore, due to the Lighthill criterion [33], the modulation instability effect in the cubic approximation is absent for this wave. In the nonlinear Schrödinger equation for a weakly nonlinear Gerstner wave, the nonlinearity coefficient becomes zero [34]. This is a consequence of the well-defined distribution of vorticity in the wave. In this regard, a question about vortex waves with a more general type of vorticity quite naturally arises.

3. GOUYON WAVES

When expanding Ω_G over the small wave steepness parameter, only the terms with even powers of ε are non-zero (see Eq. (4)). The expansion coefficients are well-defined functions of the b coordinate. However, when describing a stationary flow, the vorticity may arbitrarily depend on the variable b. Therefore, a natural generalization of the Gerstner wave will be stationary waves with vorticity of the form

$$\Omega_*(b) = \sum_{n=1}^{\infty}\varepsilon^n\Omega_n(b), \tag{6}$$

where the vortices of the nth approximation Ω_n can arbitrarily be chosen. For the first time this question was studied by Dubreil-Jacotin [35], but Gouyon considered it in a more complete form [7, 36]. Both researchers used Eulerian coordinates (in this case, the current function should be written instead of the variable b in

Eq. (6)). Gouyon, having considered the problem up to the quadratic approximation, found a correction proportional to ε to the propagation velocity of a linear wave. We will refer to the oscillations of a fluid with vorticity (6) as Gouyon waves. Below, Gouyon's result will be reproduced in Lagrange variables and generalized to the cubic approximation.

Consider a stationary plane wave traveling in the positive direction of the X axis. Let us write the equations of two-dimensional hydrodynamics (1) in the following form:

$$X_a Y_b - X_b Y_a = 1, \tag{7}$$

$$X_{tt} = -H_a Y_b + H_b Y_a; \qquad Y_{tt} = -H_b X_a + H_a X_b; \qquad H = p/\rho + gY. \tag{8}$$

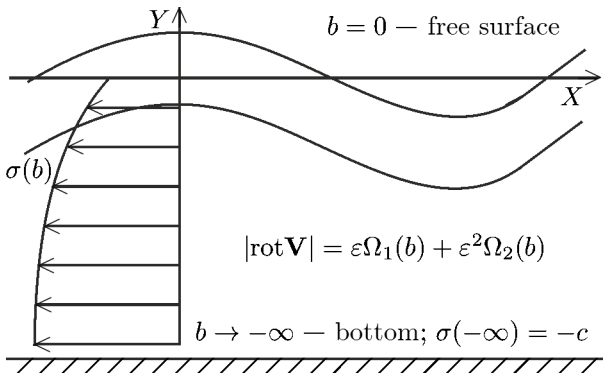

Fig. 2. The pattern of a stationary flow in the wave reference frame: periodic perturbations of a flow with the profile $\sigma(b)$.

Now the Lagrangian coordinates coincide with the initial position of the fluid particles, and $D_0 = 1$. To analyze the motion, it is convenient to switch to the reference frame moving at the wave speed c, where the flow is stationary (see Fig. 2). In Lagrange variables, two-dimensional stationary motion is represented as [26, 37]

$$X = X(q, b), \qquad Y = Y(q, b), \qquad q = a + \sigma(b)t, \tag{9}$$

where $\sigma(b)$ is some function. The simplest way to verify this is to write the velocity field (9) in Euler variables. The velocity components in the Lagrangian representation $X_t = \sigma X_q$ and $Y_t = \sigma Y_q$, as well as the functions X and Y themselves, depend only on the variables q and b; therefore, the Eulerian velocity field $X_t(X, Y)$, $Y_t(X, Y)$ does not depend on time. We emphasize that the q coordinate is not a marker of a fluid particle, which means that this approach is no longer Lagrangian. The relationship between the function $\sigma(b)$ and the wave velocity is shown in Fig. 2 and will be explained below. The coordinates q and b were first introduced in [37] and called modified Lagrangian coordinates [26].

In the new variables, the system of equations (7) and (8) takes the form

$$X_q Y_b - X_b Y_q = 1, \tag{10}$$

$$\sigma^2 X_{qq} = -H_q Y_b + H_b Y_q; \qquad \sigma^2 Y_{qq} = -H_b X_q + H_q X_b. \tag{11}$$

Assume that $X = q + \xi$ and $Y = b + \eta$, where the functions ξ and η have the meaning of periodic deviations of the trajectory coordinates of a fluid particle from the modified Lagrangian coordinates. Equations (10) and (11) will be rewritten as

$$\xi_q + \eta_b = -\frac{D(\xi, \eta)}{D(q, b)}, \qquad \sigma^2 \xi_{qq} = -H_q + \frac{D(\eta, H)}{D(q, b)}, \qquad \sigma^2 \eta_{qq} = -H_b - \frac{D(\xi, H)}{D(q, b)}. \tag{12}$$

Equations (12) are supplemented by the following boundary conditions. At the bottom, the vertical velocity becomes zero:

$$Y_t = \sigma Y_q = \sigma \eta_q \to 0 \quad at \quad b \to -\infty;$$

on a free surface, the pressure is constant:

$$H(q, 0) - g\eta(q, 0) = p_0/\rho = \text{const};$$

the position of the mean fluid level on the horizon $Y = 0$ is unchanged:

$$\int_0^\lambda Y \, \mathrm{d}X \bigg|_{b=0} = \int_0^\lambda \eta(1 + \xi_q) \, \mathrm{d}q \bigg|_{b=0} = 0,$$

where $\lambda = 2\pi/k$ is the wavelength. Since the fluid is deep, it should be natural to assume that no wave disturbances take place at the bottom and the horizontal velocity is also absent. Herein, the flow is described by the expressions $X = q$ and $Y = b$, which specify a shear current with the velocity profile $\sigma(b)$. The velocity at the bottom is then equal to the wave velocity with the opposite sign: $\sigma(-\infty) = -c$. This means that in the laboratory reference frame, the bottom velocity is zero. The difference between the shear current velocity and the bottom velocity determines the drift of fluid particles

$$u(b) = \sigma(b) - \sigma(-\infty) = \sigma(b) + c.$$

The vorticity expression with allowance for Eq. (7) is represented as

$$\Omega = \frac{\partial Y_t}{\partial X} - \frac{\partial X_t}{\partial Y} = \frac{D(X_t, X)}{D(X, Y)} + \frac{D(Y_t, Y)}{D(X, Y)} = \frac{D(X_t, X)}{D(a, b)} + \frac{D(Y_t, Y)}{D(a, b)} = \frac{D(\sigma X_q, X)}{D(q, b)} + \frac{D(\sigma Y_q, Y)}{D(q, b)},$$

or after switching to the functions ξ and η

$$\Omega = -\sigma'(1 + 2\xi_q) + \sigma(\eta_{qq} - \xi_{qb}) + \frac{D(\sigma\xi_q, \xi)}{D(q, b)} + \frac{D(\sigma\eta_q, \eta)}{D(q, b)}. \tag{13}$$

Hereafter, the primes denote a derivative of the function by its argument. For the stationary flow (9), the vorticity depends only on the b coordinate.

We will focus on weakly nonlinear wave motion. Let us introduce expansions of the desired functions and quantities in a series over the small wave steepness parameter

$$\{\xi, \eta, u, H\} = \sum_{n=1}^{\infty} \varepsilon^n \{\varepsilon_n, \eta_n, u_n, H_n\}; \qquad c = \sum_{n=0}^{\infty} \varepsilon^n c_n; \qquad \sigma = \sigma_0 + \sum_{n=1}^{\infty} \varepsilon^n \sigma_n$$

and substitute into Eqs. (12). The properties of Gouyon waves for the first three approximations were studied in [38].

The coordinates of the trajectories of fluid particles in the Gouyon linear wave in Lagrangian variables are written as

$$\begin{gathered} X = a - c_0 t + \varepsilon\sigma_1(b)t - \varepsilon(1/k)\exp(kb)\sin k[a - c_0 t + \varepsilon\sigma_1(b)t]; \\ Y = b + \varepsilon(1/k)\exp(kb)\cos k[a - c_0 t + \varepsilon\sigma_1(b)t], \end{gathered} \tag{14}$$

where $c_0 = \sqrt{g/k} = \sigma_0$. The propagation velocity c_0 of the wave coincides with the phase velocity of linear potential waves. In addition to the oscillatory motion, the particles participate in inhomogeneous drift, determined by the form of the function $\sigma_1(b)$. It follows from Eq. (13) that $\sigma_1' = -\Omega_1$, i. e.,

$$\sigma_1(b) = \sigma_1(-\infty) - \int_{-\infty}^{b} \Omega_1(b)\,\mathrm{d}b = -c_1 - \int_{-\infty}^{b} \Omega_1(b)\,\mathrm{d}b. \tag{15}$$

As can be seen, the vorticity $\Omega_1(b)$ does not fully define the function $\sigma_1(b)$. In the first approximation, it is obtained with accuracy up to the constant (linear correction to c_0, taken with the reverse sign). Its value is set in the next approximation. This feature will also be preserved for higher-order corrections. The integral term in Eq. (15) corresponds to the drift velocity of fluid particles

$$u_1(b) = \sigma_1(b) + c_1 = -\int_{-\infty}^{b} \Omega_1(b)\,\mathrm{d}b.$$

In each approximation, vorticity determines the drift motion of particles, but the correction to the propagation velocity should be obtained from the equations of the next order of perturbation theory.

TABLE 1. Properties of the considered triad of waves in the linear approximation. The minus and plus signs denote the absence and presence of the corresponding characteristic.

Characteristic	Stokes wave	Gerstner wave	Gouyon wave
Vorticity	−	−	+
Drift current	−	−	+
Particle trajectories in a laboratory reference frame	circles	circles	loop lines

In the laboratory reference frame, the solution of a linear problem has the form

$$X = a + \varepsilon[\sigma_1(b) + c_1]t - \varepsilon(1/k)\exp(kb)\sin k[a - c_0 t + \varepsilon\sigma_1(b)t];$$
$$Y = b + \varepsilon(1/k)\exp(kb)\cos k[a - c_0 t + \varepsilon\sigma_1(b)t]. \tag{16}$$

The wave moves to the right with speed $c_0 + \varepsilon c_1$. For $\sigma_1 = 0$ and $c_1 = 0$ (vorticity is absent), Eqs. (16) describe a linear Stokes wave and a Gerstner wave of low steepness.

For the Gouyon wave, the speed $\sigma_1(b) \neq 0$ (and is not constant); therefore, fluid particles, along with the circular rotation, participate in a drift inhomogeneous in depth, so that their trajectories represent loop lines. If $\sigma_1(b) + c_1 > 0$, the particles move parallel to the wave, and anti-parallel if the sign of the inequality is reverse. The properties of the wave triad in the linear limit are compared in Table 1. The differences between Gouyon waves and the other two models are obvious.

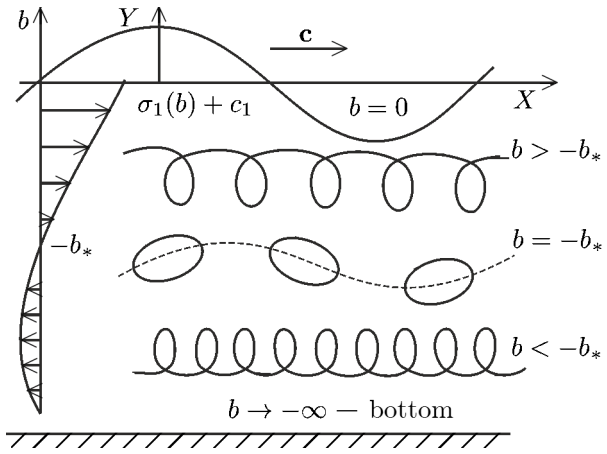

Fig. 3. Trajectories of fluid particles in a Gouyon linear wave in a laboratory reference frame for a flow with the profile $\sigma_1(b)+c_1 = \alpha(b+b_*)\exp(\beta b)$, $b_* > 0$.

The function $\sigma_1(b)$ in solution (16) describes the shear current. Due to the arbitrary choice of $\Omega_1(b)$ the profile of this current can also be arbitrary. In particular, the profile $\sigma_1(b)$ may have a cusp. As is known, linear waves on the surface of the current $\sigma_0(b)$ having a cusp are unstable [39]. In the case considered, $\sigma_0 = \text{const}$ and the profile $\sigma_1(b)$ can be arbitrary. For example, let us choose it in the form

$$\sigma_1(b) + c_1 = \alpha(b + b_*)\exp(\beta b), \qquad b_* > 0,$$

where the constant α has a velocity dimension and the constant β, an inverse-length dimension ($\alpha, \beta > 0$). The current is directed along the X axis for particles with coordinates $b > -b_*$ and anti-parallel the axis in the case of the opposite inequality. At the point $b = -b_* - 2/\beta$, the profile has a cusp (Fig. 3). In the laboratory reference frame, the particles located on the horizon $b = -b_*$ move along a circle and on the higher and lower horizons, along loop lines, while the particle drift directions relative to this horizon are different.

As a result of the solution in quadratic and cubic approximations, the following corrections to the wave velocity are obtained [38]:

$$c_1 = -\int_{-\infty}^{0} [1 - \exp(2kb)]\Omega_1(b)\,\mathrm{d}b;$$
$$c_2 = \frac{1}{2}c_0 - \int_{-\infty}^{0} [1 - \exp(2kb)]\Omega_2(b)\,\mathrm{d}b. \tag{17}$$

Equation (17) was previously obtained by Gouyon in Euler variables [7, 36]. Our calculations generalize Gouyon's result. It is noteworthy that the quadratic correction to the linear propagation velocity depends only on the quadratic vorticity Ω_2. For $\Omega_1 = \Omega_2 = 0$, we obtain the Stokes result and for $\Omega_1 = 0$ and $\Omega_2 = \Omega_{G2}$ (see Eq. (4)), Gerstner's result. In the case $\Omega_1 = 0$ and $\Omega_2 \neq 0$, a nonlinear Schrödinger equation can be derived for the Gouyon wave packet [38].

4. GENERALIZED GERSTNER WAVES

In the theory of water waves, the pressure on a free surface is conventionally assumed to be constant. However, this condition can be violated in the presence of wind. Its effect can be taken into account as the action of inhomogeneous and non-stationary pressure on a free surface.

Consider the fluid motion in the XY plane. We introduce complex coordinates of the fluid particle trajectory $W = X + iY$, $\bar{W} = X - iY$ and complex Lagrangian coordinates $\chi = a + ib$ and $\bar{\chi} = a - ib$. In this case, the system of equations (1) and (4) can be written as a condition of time independence of two Jacobians [26, 40, 41]:

$$\frac{\partial}{\partial t}\frac{D(W,\bar{W})}{D(\chi,\bar{\chi})} = 0; \qquad \frac{\partial}{\partial t}\frac{D(W_t,\bar{W})}{D(\chi,\bar{\chi})} = 0. \tag{18}$$

By direct calculation it can be shown that

$$W = G(\chi)\exp(i\lambda t) + F(\bar{\chi})\exp(i\mu t), \tag{19}$$

where G and F are analytical functions, and λ and μ are real numbers, is an exact solution to system (18). The functions G and F are largely arbitrary, since the only restriction on their choice is the requirement that the expression $|G'|^2 - |F'|^2$ does not become zero in the current region.

In the flows (19), the particle moves in a circle with radius $|F|$, the center of which rotates along a circle with radius $|G|$. If the ratio of frequencies μ and λ is positive, the trajectory of the particle is an epicycloid and if negative, a hypocycloid, and the number of loops on the curve depends on the frequency ratio. The planets moved in such orbits in the Ptolemaic picture of the world; therefore, these flows were called Ptolemaic [40, 41].

The Gerstner wave belongs to the class of Ptolemaic flows. It is described by the expression $W = \chi + iA\exp[i(k\bar{\chi} - \omega t)]$; $\mathrm{Im}\chi \leq 0$. The pressure on the Gerstner wave profile is constant. However, this condition can be violated if wind is present. Wind effect can be modeled by specifying the inhomogeneous and non-stationary pressure distribution on a free surface. Thus, the problem is reduced to studying the effect of boundary conditions of this type on the wave evolution.

Within the framework of this approach, we will consider generalizations of Gerstner waves. Assume that the flow region in Lagrangian variables corresponds to a lower half-plane, and it is described by the expression

$$W = G(\chi) + F(\bar{\chi})\exp(-i\omega t). \tag{20}$$

This motion belongs to a family of Ptolemaic flows, but, in contrast to the Gerstner wave, the function G may differ from the linear one, and the F function, from the exponent. The function G specifies the level relative to which the particles of a free surface rotate, and the modulus of the function F determines the radius of their circular rotation (wave amplitude). The fluid is at rest at depth; thus, the corresponding condition has the form

$$|F| \to 0 \quad \text{at} \quad b \to -\infty.$$

Since the function is analytical, it reaches the maximum on a free surface. It follows from this that the particles located on it have the largest oscillation amplitude.

The wave solution (20) corresponds to the pressure distribution [26]

$$\frac{p - p_0}{\rho} = -g\,\mathrm{Im}[G + F\exp(-i\omega t)] + \frac{1}{2}\omega^2|F|^2 + \mathrm{Re}[\exp(i\omega t)\int \omega^2 G'\bar{F}\,\mathrm{d}\chi].$$

TABLE 2. Examples of generalized Gerstner waves (the constants α and β are different for different cases).

Wave model	$G(\chi)$	$F(\bar{\chi})$	References
Oscillating standing	χ	$\dfrac{\beta}{(\bar{\chi}+i)^n}$; $\quad\beta>0,\quad n\geq 2$	[42]
Oscillating soliton against the background of a Gerstner wave	χ	$iA\exp(ik\bar{\chi})+\dfrac{\beta}{(\chi+i)^n}$	[42]
Breather breaking on calm water	$\chi-\dfrac{i\beta}{(\chi-i)^2}$	$\dfrac{i\beta}{(\bar{\chi}+i)^2}$	[43]
Non-stationary Gerstner waves	$\chi+\dfrac{\beta}{\chi-i\alpha}$	$iA\exp(ik\bar{\chi})$	[44]
Rogue wave inside a Gerstner wave packet	$\chi+\dfrac{i}{k}\ln[1+P(\chi/\alpha)]$; $P(\chi/\alpha)=\dfrac{i\beta}{i\alpha-\chi}$	$iA[1+\overline{P(\chi/\alpha)}]\exp(ik\bar{\chi})$	[45]
Rogue wave against the background of a Gerstner wave	$\chi-\dfrac{i\beta}{(\chi-i\alpha)^2}$	$-iA\exp(ik\bar{\chi})+\dfrac{i\beta}{(\bar{\chi}+i\alpha)^2}$	[46]

In general, the pressure changes periodically over time and is inhomogeneous along the surface $\mathrm{Im}\chi=0$. In fact, we have found a whole class of exact solutions that describe the complex dynamics of a free boundary in the case of inhomogeneous and harmonically varying pressure on it. The vorticity of the waves (35) is given by the formula $\Omega=2\omega\,|F'|^2/(|F'|^2-|G'|^2)$. In the general case, it is a complex function of Lagrange variables.

Various examples of generalized Gerstner waves (19) have been studied in a series of papers [42–46]. Their characteristics are presented in Table 2. Ptolemaic solutions allow one to analyze a number of non-stationary phenomena. Consider two examples.

4.1. Breather breaking [43]

The breather dynamics on calm water is shown in Fig. 4. Solution (19) with the functions G and F corresponding to the third row in Table 2, evolves differently depending on the value of β. Let us start the analysis with $t_0=\pi/\omega$. At this moment, the shape of the free boundary is symmetrical with respect to the vertical axis passing through the point of maximum deviation (Fig. 4*a*). Its height is equal to 2β (or $2\alpha\beta$ in dimensional form). For negative β the free surface has a depression. When $\beta>0$, the profile has a pit.

Figure 4 shows the evolution of the breather during one oscillation period. The perturbation of a free surface changes shape, but does not move as a whole. Therefore, we can call it a breather. Over time, the breather profile changes. Two qualitatively different regimes are possible: the profile has no cusps for $\beta=-0.25$ or $\beta=0.50$, while for $\beta=0.85$ the profile has cusps and the breather breaks.

We focus on the profile with $\beta=0.85$ (thick lines in Fig. 4). Over time, the steepness of the leading edge increases, and at $t_1=4.25\pi/\omega$ (Fig. 4*b*) the cusp appears for the first time. This point is characterized by a vertical tangent to the profile, shown by a dotted line. Further, the profile has two cusps till the instant $t_3=5.9\pi/\omega$ when they merge, and then the cusp disappears. At the instant $t=2\pi/\omega$ the free surface becomes flat.

During the next half-cycle, all stages of evolution repeat symmetrically (Figs. 4*e*–4*g*), but the cusps are formed on the left slope of the breather. The cusp occurs at $t_4=6.7/\omega$ when the steepness is fairly low. It is hardly possible to observe such a situation in full-scale conditions. The breather dynamics during

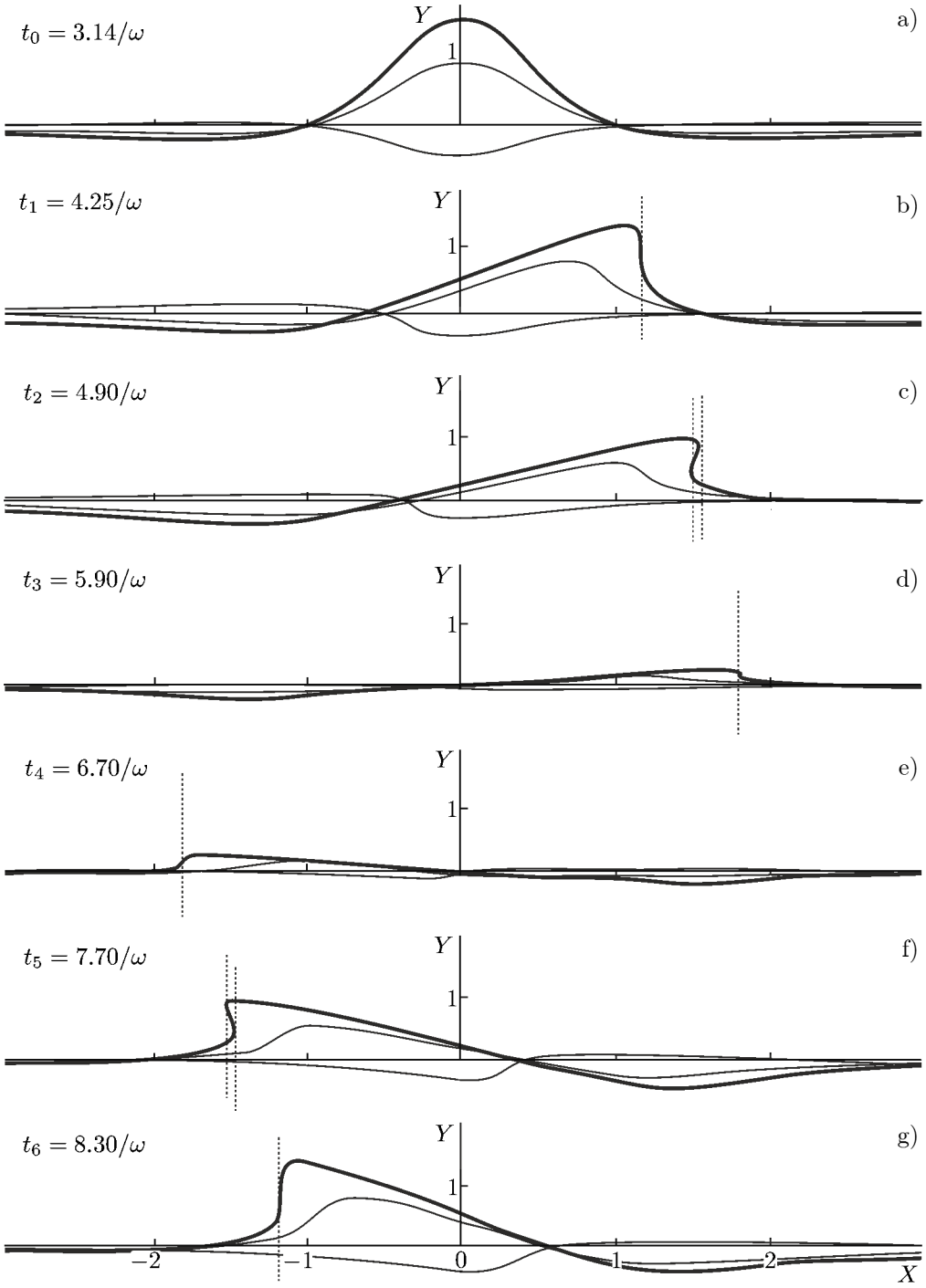

Fig. 4. Evolution of the breather profile for various values of β. Thick lines correspond to $\beta = 0.85$, black thin lines, to $\beta = 0.5$, and gray thin lines, to $\beta = -0.25$. The X and Y coordinates are normalized by the α value.

the first half-cycle is very similar to the breaking of ocean waves. Closer to the time when the vertical tangent appears on the profile, it is necessary to take into account the viscosity effect, which will destroy the considered solution at some instant $t_* > t_1$. Thus, Eq. (20) describes the wave breaking in the interval (t_0, t_*). For example, one can choose $t_* = t_2$.

It is worth recalling and emphasizing that Eq. (20) corresponds to an inhomogeneous and non-stationary distribution of pressure on a free surface. The pressure oscillates antiphase with profile oscillations.

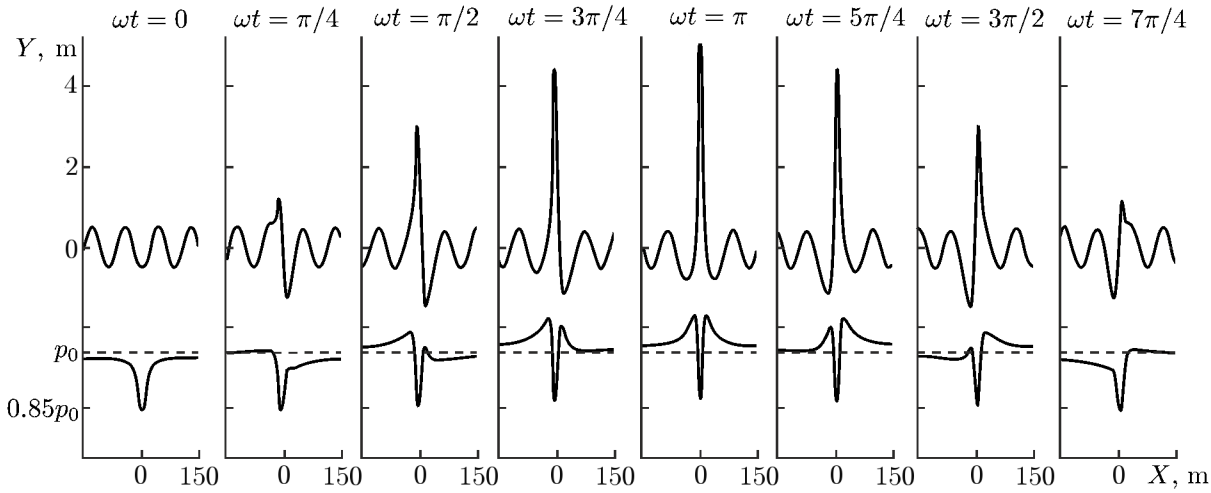

Fig. 5. Formation of a rogue wave against the background of a Gerstner wave.

4.2. Rogue wave against the background of a Gerstner wave [46]

Figure 5 shows the wave surface dynamics for Eq. (20) with the functions G and F corresponding to the formulas in the last line in Table 2. The calculation was performed for the case $A = 0.5$ m; $k = 0.074$ m^{-1}, $\alpha = 12$ m, and $\beta = 328$ m^3; $\omega = \sqrt{gk} = 0.85$ s^{-1} and $\lambda = 84.9$ m. At the initial moment ($t = 0$), the free surface shape (upper curve) exactly coincides with the Gerstner wave profile. Later on, a peak begins to grow on the profile, which at the instant $t = \pi/\omega$ reaches its maximum and subsequently decreases and disappears by the end of the period. The greatest peak height $h = (2\beta/\alpha^2) + A \approx 5.1$ m. This value exceeds the Gerstner wave amplitude A by eight times. Therefore, the formation of a peak can be considered as the formation of a rogue wave (for more information on the rogue-wave phenomenon see [47]). The reason is the pressure acting at the border. The lower curve in Fig. 5 shows the deviation of the free-surface pressure from the atmospheric pressure p_0. At each point of the surface the deviation changes with time, but its negative drop in the wave peak area is about 100 mm Hg.

5. CONCLUSIONS

We review the analytical results of the Lagrangian description of vortex gravity surface waves. The theory of stationary low-vorticity waves in deep water (Gouyon waves) is discussed. Their comparison with the Gerstner wave and the Stokes wave is performed. The derivation of exact solutions in Lagrange variables (Ptolemaic flows) demonstrating the complex dynamics of nonlinear vortex waves under the action of external pressure on a free surface is given. As examples, the evolution of a single breather on calm water and the formation of a rogue wave against the background of a Gerstner wave are analyzed.

The work by E. N. Pelinovsky was supported by the Russian Science Foundation (project No. 19–12–00253).

REFERENCES

1. J. S. Russell, in: *Rept. 14th Meetings of the British Assoc. for the Advancement of Science*, John Murray, London (1844).
2. D. J. Korteweg and G. de Vries, *Phil. Mag.*, **39**, 422–443 (1895).
3. F. Gerstner, *Ann. Phys. Lpz.*, **32**, No. 2, 412–415 (1809).
4. H. Lamb, *Hydrodynamics*, Cambridge University Press, Cambridge (1916).

5. G. G. Stokes, *Cambridge Trans.*, **8**, 441–473 (1847).
6. A. N. Kriloff, *Trans. Inst. Naval. Archit.*, **40**, 135–196 (1898).
7. L. N. Sretenskiy, *Theory of Wave Motions of a Fluid* [in Russian], Nauka, Moscow (1977).
8. M. L. Dubreil-Jacotin, *Atti. Accad. Lincei. Rend. Cl. Sci. Fis. Mat. Nat.*, **6**, No. 15, 814–819 (1932).
9. T. B. Benjamin, *J. Fluid Mech.*, **27**, No. 3, 417–430 (1967). https://doi.org/10.1017/S002211206700045X
10. R. T. Pollard, *J. Geophys. Res.*, **75**, No. 30, 5895–5898 (1970). https://doi.org/10.1029/JC075i030p05895
11. C.-S. Yih, *J. Fluid Mech.*, **24**, 765–767 (1966). https://doi.org/10.1017/S0022112066000983
12. E. Mollo-Christensen, *Phys. Fluids*, **25**, No. 4, 586–587 (1982). https://doi.org/10.1063/1.863802
13. E. Mollo-Christensen, *J. Phys. Ocean*, **9**, No. 1, 226–229 (1978). https://doi.org/10.1175/15200485(1979)009<0226:EWIARS>2.0.CO;2
14. A. Constantin, *J. Phys. A: Maths. Gen.*, **34**, No. 45, 9723–9731 (2001). https://doi.org/10.1088/03054470/34/45/311
15. E. Mollo-Christensen, *J. Atm. Sci.*, **35**, No. 8, 1395–1398 (1978). https://doi.org/10.1175/1520-0469(1978)035<1395:GAGBSE>2.0.CO;2
16. N. A. Inogamov, *Sov. Phys. Dokl.*, **29**, No. 9, 714–716 (1984).
17. A. A. Abrashkin, *Prikl. Mekh. Tekhn. Fiz.*, No. 3, 86–88 (1984).
18. S. G. Monismith, E. A. Cowen, H. M. Nepf, et al., *J. Fluid Mech.*, **573**, 131–147 (2007). https://doi.org/10.1017/S0022112006003594
19. C. Swan, in: *Proc. 22nd Intl. Coastal Engng. Conf., July 2–6, 1990, Delft, The Netherlands*, pp. 489–502.
20. J. Y. Jiang and R. L. S. Street, *J. Geophys. Res. Oceans*, **96**, No. C2, 2711–2721 (1991). https://doi.org/10.1029/90JC02259
21. L. Thais, *Contribution a L'ètude du Movement Turbulent sous des Vagues de Surface Cisaillèes par le Vent*, Thèse Inst. Nat. Polytech., Toulouse (1994).
22. J. A. Smith, *J. Phys. Oceanogr.*, **36**, No. 7, 1381–1402 (2006). https://doi.org/10.1175/JPO2910.1
23. S. Leblanc, *J. Fluid Mech.*, **506**, 245–254 (2004). https://doi.org/10.1017/S0022112004008444
24. J. E. H. Weber, *Wave Motion*, **48**, No. 4, 301–309 (2011). https://doi.org/10.1016/j.wavemoti.2010.11.005
25. N. E. Kochin, I. A. Kibel', and N. V. Roze, *Theoretical Hydromechanics*, John Wiley & Sons Ltd, Chichester (1964).
26. A. A. Abrashkin and E. I. Yakubovich, *Lagrangian Description of Vortex Dynamics* [in Russian], Fizmatlit, Moscow (2006).
27. A. Bennett, *Lagrangian Fluid Dynamics*, Cambridge University Press, Cambridge (2006).
28. W. Froude, *Trans. Inst. Naval. Arch.*, **3**, 45–62 (1862).
29. W. J. M. Rankine, *Phil. Trans. R. Soc. Lond. A*, **153**, 127–138 (1863).
30. F. C. R. Reech, *Acad. Sci. Paris*, **68**, 1099–1101 (1869).
31. D. Clamond, *J. Fluid Mech.*, **589**, 433–454 (2007). https://doi.org/10.1017/S0022112007007811
32. A. A. Abrashkin and E. N. Pelinovsky, *Phys. Usp.*, **61**, No. 3, 307–312 (2018). https://doi.org/10.3367/UFNe.2017.03.038089
33. M. J. J. Lighthill, *Inst. Math. Appl.*, **1**, No. 3, 269–306 (1965).

34. A. Abrashkin and E. Pelinovsky, *Nonl. Proc. Geoph.*, **24**, No. 2, 255–264 (2017). https://doi.org/10.5194/npg24-255-2017

35. M. L. Dubreil-Jacotin, *J. Math. Pures Appl. Ser. 9*, **13**, 217–291 (1934).

36. R. Gouyon, *Ann. de la Facultè des Sciences de l'Universitè de Toulouse. Ser. 4*, **22**, 1–55 (1958).

37. A. A. Abrashkin and D. A. Zen'kovich, *Izv. Akad. Nauk USSR*, **26**, No. 1, 35–45 (1990).

38. A. A. Abrashkin and E. N. Pelinovsky, *J. Phys. A: Math. Theor.*, **54**, 395701 (2021). https://doi.org/10.1088/1751-8121/ac1f3e

39. P. G. Drazin, *Intoduction to Hydrodynamic Stability*, Cambridge University Press, Cambridge (2002).

40. A. A. Abrashkin and E. I. Yakubovich, *Sov. Phys. Dokl.*, **29**, 370–374 (1984).

41. A. A. Abrashkin and E. I. Yakubovich, *Prikl. Mekh. Tekhn. Fiz.*, No. 2, 57–64 (1985).

42. A. A. Abrashkin and A. G. Solov'ev, *Fluid Dyn.*, **48**, No. 5, 679–686 (2013). https://doi.org/10.1134/S0015462813050116

43. A. Abrashkin and O. Oshmarina, *Phys. Lett. A*, **378**, 2866–2871 (2014). https://doi.org/10.1016/j.physleta.2014.08.009

44. A. A. Abrashkin, *Chaos Solit. Fractals*, **118**, 152–158 (2019). https://doi.org/10.1016/j.chaos.2018.11.007

45. A. A. Abrashkin and O. E. Oshmarina, *Commun. Nonl. Sci. Num. Simul.*, **34**, 66–76 (2016). https://doi.org/10.1016/j.cnsns.2015.10.006

46. A. A.Abrashkin and A. Soloviev, *Phys. Rev. Lett.*, **110**, 014501 (2013). https://doi.org/10.1103/PhysRevLett.110.014501

47. S. Kharif, E. Pelinovsky, and A. Slunyaev, *Rogue Waves in the Ocean*, Springer–Verlag, Heidelberg, Berlin (2009).